

Document Version

Accepted author manuscript

Citation (APA)

Wang, H., Liu, X., Apostolidis, P., Erkens, S., & Skarpas, A. (2020). Experimental Investigation of Rubber Swelling in Bitumen. *Transportation Research Record*, 2674(2), 203-212. <https://doi.org/10.1177/0361198120906423>

Important note

To cite this publication, please use the final published version (if applicable).
Please check the document version above.

Copyright

In case the licence states "Dutch Copyright Act (Article 25fa)", this publication was made available Green Open Access via the TU Delft Institutional Repository pursuant to Dutch Copyright Act (Article 25fa, the Taverne amendment). This provision does not affect copyright ownership.
Unless copyright is transferred by contract or statute, it remains with the copyright holder.

Sharing and reuse

Other than for strictly personal use, it is not permitted to download, forward or distribute the text or part of it, without the consent of the author(s) and/or copyright holder(s), unless the work is under an open content license such as Creative Commons.

Takedown policy

Please contact us and provide details if you believe this document breaches copyrights.
We will remove access to the work immediately and investigate your claim.

Experimental Investigation of Rubber Swelling in Bitumen

Haopeng Wang¹, Xueyan Liu¹, Panos Apostolidis¹, Sandra Erkens¹, Athanasios Skarpas^{2,1}

¹Section of Pavement Engineering, Faculty of Civil Engineering & Geosciences, Delft University of Technology, Delft, The Netherlands

²Department of Civil Infrastructure and Environmental Engineering, Khalifa University, Abu Dhabi, United Arab Emirates

Corresponding author: Haopeng Wang

Email: haopeng.wang@tudelft.nl

[ORCID: 0000-0002-5008-7322](https://orcid.org/0000-0002-5008-7322)

Word count:

Word in abstract	=	231	words
Words in text	=	5420	words
Tables (2)	=	500	words equivalent
<hr/> Total	=	<hr/> 6151	<hr/> words equivalent

Funding

The corresponding author would like to thank the financial support from China Scholarship Council. The financial support of Khalifa University via the CIRA-2018-115 research grant is also gratefully acknowledged.

Data Accessibility Statement

The datasets generated during and/or analyzed during the current study are available from the corresponding author on reasonable request.

1 ABSTRACT

2 Rubber swelling in bitumen, which is a diffusion-induced volume expansion process, plays a dominant role
3 in the design of crumb rubber modified bitumen (CRMB) binders and their properties development. This
4 study aims to investigate the kinetics of bitumen diffusion into truck tire rubber, the equilibrium swelling
5 characteristics of rubber and the mechanical properties of rubber before and after swelling at different high
6 temperatures. Fourier transform infrared spectroscopy (FTIR) results indicate that no rubber dissolution
7 happens during the interaction in the temperature range from 160 to 200 °C. Aliphatic compounds from
8 bitumen preferentially diffused into rubber during the swelling process. The diffusion coefficients of
9 bitumen into rubber were determined by the sorption test using the gravimetric method. The diffusion
10 coefficient increases with the increase of temperature in an Arrhenius form. The volume expansion of rubber
11 during swelling was captured by the X-ray computed tomography (CT) scan images. Rubber swells faster
12 at the earlier stages then the expansion rate slows down. The swelling ratio of rubber increased from 1.97 at
13 160 °C to 3.03 at 200 °C after 36 h interaction. Mechanical tests by dynamic shear rheometer (DSR) reveal
14 that swollen rubber becomes softer comparing to the dry rubber and exhibits obvious viscoelastic behaviors.
15 With the increase of temperature, the softening and viscous effect are more significant. The obtained
16 parameters can be implemented to swelling and micromechanical models to better predict the binder
17 properties.

18
19
20
21
22

Keywords: Crumb rubber modified bitumen, Swelling, Diffusion, Mechanical property

1 INTRODUCTION

2 The use of crumb rubber modified bitumen (CRMB) has become a common practice in the asphalt paving
3 industry for many years. Modification of bitumen with crumb rubber modifiers (CRMs) from scrap tires
4 was reported to improve the physical and mechanical properties of binders. Comparing to neat bitumen,
5 CRMB has higher resistance to rutting, aging, fatigue and thermal cracking (1-3). These improvements are
6 attributable to the interaction between bitumen and CRM.

7 Bitumen, as a refined residue from the distillation process of crude oils, is a complex mixture of thousands
8 of different hydrocarbon molecules. Based on the differences in size and polarity, bitumen molecules can
9 be separated into four molecular groups, saturates, aromatics, resins and asphaltenes (SARA). Bitumen is
10 commonly accepted as a multi-disperse colloidal system, where high-molecular-weight asphaltene micelles
11 are peptized by resins and dispersed in low-molecular-weight maltenes (saturates and aromatics) (4). CRM
12 mainly consists of natural and synthetic rubber, which are cross-linked with sulfur and reinforced with
13 carbon black. In addition, various processing agents, such as aromatic hydrocarbons and antioxidants, have
14 been added to improve its workability and prevent it from aging, respectively (5). The often-referred
15 interaction during the production of CRMB in literature is essentially the interaction between the rubber
16 polymer and bitumen. From the viewpoint of polymer science, the bitumen-rubber interaction can be
17 regarded as a process that a polymer (rubber) dissolves into a low-molecular-weight solvent (bitumen).
18 Depending on different interaction parameters (e.g., temperature, time and mixing technique, etc.) (6-8),
19 there are two mechanisms involved in the bitumen-rubber interaction process: diffusion-induced swelling
20 of rubber network and chain disentanglement/secession of the swollen rubber (rubber degradation) (9).
21 Theoretically, swelling and degradation are two successive processes of the dissolution of rubber in bitumen.
22 As elastomers, rubber particles swell by absorption of the aromatic oils from the bituminous matrix to form
23 a gel-like structure at elevated temperatures. After the completion of rubber swelling and under severe
24 interaction conditions (excessively high mixing temperature with high shear and extended mixing time),
25 rubber network degradation occurs. This process involves two chemical reactions: depolymerization and
26 devulcanization, which break down the polymer chain bonds or crosslinking bonds reducing thus the
27 average molecular weight of rubber (10). Besides the interaction conditions, the raw material parameters
28 (e.g., bitumen microstructure and composition, rubber composition, morphology and particle size, etc.) also
29 have great impacts on the dissolution process of rubber in bitumen.

30 Few studies in the past have been done to quantitatively investigate the diffusion of bitumen into rubber.
31 Frantzis measured the mass uptake of rubber in bitumen to determine the diffusion and solubility coefficients
32 of bitumen in rubber from waste tires at 180 °C (11). Artamendi and Khalid extended this gravimetric
33 method to different types of bitumen to investigate the diffusion kinetics (12). More recently, Dong et al.
34 used the SBR sheet to simulate the swelling process of rubber in bitumen. Differential scanning calorimetric
35 analysis, X-ray photoelectron spectroscopy tests, infrared spectroscopic analysis, and tensile tests were
36 conducted to examine the physical, chemical and mechanical properties of rubber before and after swelling
37 in rubber (13).

38 The bitumen-rubber interaction alters not only the component fractions and microstructure of bitumen but
39 also the nature of rubber. Rubber swelling process stiffens the binder while degradation is detrimental to the
40 mechanical properties of binder. For the conventional wet-processed CRMB at temperatures from 160 °C
41 to 200 °C, only partial degradation occurs, and the final binder properties are dominated by the rubber
42 swelling process (9). Therefore, it is of vital importance to understand the interaction process to guide the
43 production of CRMB. Instead of investigating the properties of CRMB prepared at different conditions with
44 different material combinations, this study focuses on the interaction between a single rubber unit and
45 bitumen at different conditions. It is not the intention of this study to involve many material combinations,

1 but instead, to develop a robust methodology to determine the diffusion kinetics of bitumen into rubber and
2 swelling properties of rubber.

3 **OBJECTIVE AND APPROACH**

4 This study aims to investigate the kinetics of bitumen diffusion into cylindrical rubber samples cut from
5 scrap truck tires, the equilibrium swelling characteristics of rubber and the mechanical properties of rubber
6 before and after swelling at different high temperatures. From the physical viewpoint, rubber swelling is a
7 multiphysics phenomenon which consists of mass diffusion and volume expansion (mechanical
8 deformation). Gravimetric method (weight gain experiments) was used to determine mass uptake
9 parameters and diffusion coefficient. Fourier transform infrared spectroscopy (FTIR) was employed to
10 detect the component exchanges between rubber and solvent. The volume change of rubber during the
11 swelling process was measured by micro X-ray computed tomography (CT) scan. Furthermore, the
12 mechanical properties of rubber before and after swelling were tested by the dynamic shear rheometer (DSR)
13 with dedicated sample preparation procedures.

14 **MATERIALS AND METHODS**

15 **Materials and Sample Preparation**

16 Penetration grade 70/100 bitumen (Nynas) with a SARA (saturated hydrocarbons, aromatic hydrocarbons,
17 resins, asphaltenes) fraction of 7% saturates, 51% aromatics, 22% resins, and 20% asphaltenes, was used to
18 interact with the rubber. The cylindrical rubber samples were cut from waste truck tires as shown in Figure
19 1. A uniform rubber slice of 2 mm thickness was cut from the tire tread (metal fiber free) using the water
20 jet cutting technology. Then, laser cutting was applied on the slice to obtain the rubber cylinders with a
21 diameter of 8 mm. These cylindrical rubber samples were subjected to the swelling test and DSR test later.
22 The rubber sample comprises about 55% total rubber polymer (natural and synthetic rubber), 25% carbon
23 black and 20% processing agents. The processing agents mainly consist of antioxidants/antiozonants and
24 curing additives (e.g., sulfur, zinc oxide, stearic acid, accelerator and oil etc.).

25 **Rubber Swelling Test**

26 Gravimetric method (weight gain experiments) was used to determine mass uptake parameters and diffusion
27 coefficient. The cylindrical rubber samples were immersed in small glass bottles containing approximately
28 5 g bitumen. The receptacles with lid were kept in an oven at the desired temperatures of 160, 180 and
29 200 °C, which are in the temperature range of conventional wet process. At regular time intervals (0.5, 1, 2,
30 3, 4, 6, 8, 18, 24, 28, 36 h) the samples were taken out of the bottles, blotted with Kimwipes (wiped dry with
31 absorbent paper) to remove the surface-adhered excess bitumen. More dense data collection was conducted
32 at the early stages where bitumen diffusion is usually faster than later stages. The rubber samples were then
33 weighed (± 0.05 mg) on an electronic balance under closed environments. The mass uptake was obtained
34 by difference between the initial weight and the weight after immersion in bitumen. For each temperature,
35 three rubber replicates were used for the test.

36 Concurrently, another group of rubber swelling tests were performed using the same setup at the same
37 elevated temperatures of 160, 180 and 200 °C. After swelling for different time durations (2, 6, 14, 26, 36
38 h), instead of taking out the rubber samples, the glass bottles containing both rubber cylinder and bitumen
39 were scanned by the micro X-ray CT with a high resolution of 0.025 mm in all directions (Figure 2). As a
40 non-destructive visualizing technique, X-ray CT can distinguish the rubber part and the bitumen part in the
41 glass bottle based on the density difference, and thereof monitor the volume change of rubber during
42 swelling. After obtaining the 2D CT scan images, Simpleware® software was utilized to analyze the image
43 data and to reconstruct the 3D images of rubber samples for further volume calculation.

1 **DOES THE RUBBER DISSOLVE INTO BITUMEN? STUDY OF RUBBER IN NAPHTHENIC OIL**

2 Before conducting the rubber swelling test in bitumen, a question needs to be answered to ensure the results
3 obtained from the swelling tests are the consequences of swelling—does the rubber dissolve into bitumen?
4 Therefore, the rubber samples were first immersed in a naphthenic oil at elevated temperatures to examine
5 if there is dissolution of rubber taking place during the swelling process. The naphthenic oil has a Hildebrand
6 solubility parameter of $18.5 \text{ MPa}^{0.5}$, which is closer to truck tire rubber ($18.6 \text{ MPa}^{0.5}$) than most bitumen
7 components (in the range from 17.2 to $18.8 \text{ MPa}^{0.5}$) (12; 14; 15). Therefore, it is easier for rubber to dissolve
8 into the naphthenic oil than bitumen based on the solubility theory. The naphthenic oil was collected
9 periodically and was subjected to FTIR test to examine if there are new functional groups appear due to the
10 interaction with rubber.

11 FTIR tests were also performed on the swollen rubbers from the rubber swelling test in bitumen. Small
12 rubber units were cut from the core of swollen rubber samples with a special drill tool to avoid the
13 interference of bitumen on the surface of rubber. The small rubber units were tested by FTIR to see which
14 component of bitumen has diffused into rubber. In short, these two types of FTIR tests were performed to
15 examine what has been released into naphthenic oil and what has been diffused into rubber.

16 **Fourier Transform Infrared Spectroscopy**

17 A Perkin Elmer Spectrum 100 FTIR spectrometer was used in the attenuated total reflectance (ATR) mode
18 to acquire the infrared spectra for all the test samples. It was used to detect the component exchanges
19 between rubber and solvent. The FTIR spectrum was obtained in the wavelength number range from $4,000$
20 to 600 cm^{-1} with a scanning resolution of 4 cm^{-1} averaging twenty scans for each measurement at ambient
21 temperatures.

22 **Component Exchange between Rubber and Solvent based on FTIR Analysis**

23 As mentioned before, the objective of immersing rubber samples into the naphthenic oil at elevated
24 temperatures is to examine if the dissolution of rubber happens during the swelling process. The reason for
25 choosing a naphthenic oil instead of bitumen is because its functional groups are relatively simple compared
26 to bitumen. Besides, it is a better solvent for rubber swelling than bitumen. Therefore, it is easy to distinguish
27 if rubber polymer molecules appear in the spectra of the collected naphthenic oil samples (Figure 3a). The
28 spectrum peaks at 966 cm^{-1} and 696 cm^{-1} are often used as indicators of polybutadiene (PB) and polystyrene
29 (PS) in rubber respectively. From Figure 3a, it can be found that no rubber polymer functional groups were
30 detected as no PB or PS peaks showed up. However, the absorption peak at 1700 cm^{-1} corresponding to
31 carbonyl functional group, which was not existing in the pure naphthenic oil spectrum, appeared in the
32 reacted naphthenic oil samples. The intensity of this peak increased with higher interaction temperature and
33 extended time. This may be attributed to the released aromatic oil and oxidation of carbon black released
34 from rubber samples. Therefore, no rubber dissolution (or too inconspicuous to be detected) during
35 interaction with naphthenic oil takes place in the temperature range from 160 to $200 \text{ }^\circ\text{C}$. In addition, the
36 rubber sample retained its integrity after the interaction at a macroscale by visual inspection. It is anticipated
37 this is the same case for the interaction of rubber with bitumen based on the solubility theory. It may be
38 contradictory to previous studies which claimed the dissolution of rubber particles happened during the
39 mixing process (16). In their studies, CRM dissolution was measured by considering the portion of CRM
40 particles that passed through mesh No. 200 (smaller than 0.075 mm) as the dissolved portion. However, this
41 portion of CRMs may be the consequence of disassociation/splitting of the big particles due to the mixing
42 force and swelling effect (17). It is just a physical size-reducing process in which no dissolution happens in
43 a chemical sense. Therefore, the diffusion coefficient measured using the gravimetric method represents the
44 accurate diffusion of bitumen components into rubber since no rubber mass loss is expected.

1 Figure 3b shows the spectra of dry rubber sample and rubber samples after swelling at different temperatures.
2 It can be found that the absorption peaks at 1456 cm^{-1} and 1376 cm^{-1} corresponding to aliphatic components,
3 which were not present in the dry rubber but in the bitumen, showed up in the swollen rubber samples. The
4 two peaks close to 1456 cm^{-1} and 1376 cm^{-1} shown in the dry rubber are not related to aliphatic. This
5 indicates that aliphatic compounds from bitumen diffused into rubber during the swelling process. Previous
6 studies also observed the preferential absorption of compounds with linear aliphatic chains into rubber (18).

7 RUBBER SWELLING IN BITUMEN

8 A series of rubber swelling tests were performed at different temperatures to investigate the diffusion
9 kinetics and volume change.

10 Diffusion Coefficients of Bitumen into Rubber

11 In terms of physics, the swelling of rubber in bitumen is a diffusion-induced volume expansion phenomenon
12 (19). The driving force of the diffusion process is the chemical potential of the external solvent (maltenes)
13 produced from the concentration difference between rubber and bitumen. This diffusion process continues
14 until the concentrations of light fractions inside and outside the rubber are uniform and, consequently,
15 equilibrium swelling is reached. Fick's law of diffusion is usually used to describe the kinetics of bitumen
16 diffusion into rubber. Considering the case of one-dimensional diffusion, the total amount of diffusing
17 substance into rubber at time t can be expressed as (11):

$$\frac{M_t - M_0}{M_0} = 4 \sqrt{\frac{D}{\pi}} \cdot \frac{2\sqrt{t}}{d} \quad (1)$$

18 where M_t and M_0 are the mass of the rubber sample at immersion time t and the initial mass (g), respectively. D is
19 the diffusion coefficient (mm^2/s). d is the sample thickness (mm). Equation 1 indicates that a plot of the mass uptake
20 $(M_t - M_0)/M_0$ versus the parameter $2t^{1/2}/d$ should be initially linear. Therefore, the value of diffusion
21 coefficient, which is assumed constant, can be calculated from the slope of the initial sorption curves
22 experimentally. The initial linear region was found to be followed by a clearly defined equilibrium plateau
23 region.

24 The bitumen uptake data collected from the sorption experiments (truck tire rubber and Pen 70/10 bitumen)
25 at different temperatures are presented in Figure 4a in a plot of mass uptake versus $2t^{1/2}/d$. Each data point
26 is an average value of three replicated samples. It can be found that the bitumen components were initially
27 absorbed by rubber rapidly and then reach the equilibrium at elevated temperatures. The sorption curves
28 showed a linear region followed by an equilibrium plateau region. Furthermore, bitumen uptake was faster
29 at higher temperatures at the earlier stages as seen by the higher initial slopes of the sorption curve, which
30 indicates a higher diffusion rate. The equilibrium mass uptake also increases as the temperature increases.

31 The diffusion coefficients calculated from the initial slopes of the sorption curves and the approximate
32 equilibrium mass uptake were summarized in Table 1. The diffusion coefficients determined here were
33 considered as apparent (12) due to several reasons. First, the sample thickness was assumed as constant,
34 which in reality the thickness increased due to swelling. Second, the diffusion coefficient was assumed as
35 constant and independent of concentration (in other words, the surface concentration of penetrant is
36 constant). However, both bitumen composition and physical properties of rubber changed during the
37 diffusion process. The light fractions of bitumen diffused into rubber preferentially at the earlier stages and
38 the other fractions of bitumen might also diffuse into rubber at the later stages due to changes of the internal
39 structure of swollen rubber. Therefore, corrections to diffusion coefficients under swollen conditions were
40 made by calculating the intrinsic diffusion coefficient D^* in Equation 2 (20).

$$D^* = \frac{D}{\phi^{7/3}} \quad (2)$$

1 where ϕ is the volume fraction of rubber in the swollen condition. It can be calculated based on the densities
2 of rubber and bitumen together with the equilibrium mass uptake. The calculated equilibrium volume
3 fraction of rubber and intrinsic diffusion coefficients were also summarized in Table 1.

4 The relationship between diffusion coefficients and temperature was plot in Figure 4b. The temperature
5 dependence of the diffusion coefficient can be found to follow an Arrhenius equation (Equation 3). As the
6 temperature increases, both the mobility of bitumen molecules and polymer chains increase, which enhances
7 the diffusion process of bitumen into the rubber. Greater segmental motion results in an increase in the size
8 of free volume and subsequent increase in the diffusion coefficient (21).

$$D = D_0 e^{-\frac{E_a}{RT}} \quad (3)$$

9 where D_0 is a constant, E_a is the activation energy (kJ/mol), R is the universal gas constant [8.314
10 J/(mol·K)], T is temperature in degrees K, and D is diffusion coefficient.

11 **Volume Change of Rubber during Swelling in Bitumen**

12 X-ray CT can distinguish objects based on the difference in density and reflect them in the obtained slice
13 images with different greyscale levels. Figure 5 presents the cross-sectional images of the scanned samples
14 at different interaction conditions. The raw images were cropped to remove the glass bottle with only
15 bitumen and rubber left. The density of bitumen is 1.03 g/cm³ while the density of rubber is around 1.15
16 g/cm³. Therefore, the light part is the rubber cylinder while the surrounding dark part is bitumen. The value
17 shown in each image represents the diameter of the rubber circle using the measurement function in the
18 software. Considering the diameter of the original dry rubber sample is around 8 mm, the size of rubber
19 sample continued increasing with the increase of interaction time at different temperatures. The rubber
20 samples swell more at higher temperatures as reflected by the larger diameter. In addition, with more
21 bitumen diffuses into rubber, the rubber phase becomes darker and boundary between the two phases
22 becomes vague. Taking the image at 200 °C and 36 h as an example, it is difficult to distinguish the rubber
23 phase and bitumen phase as the greyscale values of these two phases are already very close. It shows that
24 the swollen rubber is saturated with bitumen components and may form a gel-like structure. In order to
25 quantitatively evaluate the volume change of rubber during swelling process, the 3D images of the object
26 were reconstructed with the 2D slice images. The volume of each swollen rubber was derived using the
27 built-in measurement function of the software. The volumes of the rubber samples at different swelling
28 states were summarized in Table 2. Rubber swells faster at the earlier stages then the expansion rate slows
29 down. After 36 h interaction at 160 °C, rubber swelled to twice as big as the original one. The volume of
30 rubber increased to approximately three times as the initial volume after 36 h interaction at 200 °C. Since
31 rubber swelling is a diffusion-induced volume expansion process, it is logical that higher diffusion
32 coefficients result in larger swelling ratios (swollen rubber volume divided by the dry rubber volume).

33

34 **MECHANICAL PROPERTIES CHARACTERIZATION**

35 **Mechanical Test by Dynamic Shear Rheometer**

36 The mechanical properties of rubber before and after swelling were tested by DSR. The unreacted (dry)
37 cylindrical rubber sample can be directly placed between the 8 mm parallel plates of the DSR. Before the
38 placement, a two-component adhesive, Plex 7742 and liquid Plexmon 801, was mixed and applied on the

1 surface of the bottom plate and the top surface of the rubber sample. Excess glue was removed from the
 2 sides. The test started after 10 min hardening process of the adhesive to ensure a proper bonding between
 3 rubber and plates. After CT scan, the swollen rubber samples were taken out from bitumen after swelling
 4 for 36 h, which is believed to reach the swelling equilibrium at this moment based on the diffusion test. The
 5 swollen rubber samples were cleaned from bitumen by wiping with absorbent paper while hot and brushing
 6 for a few seconds with cold trichloroethylene gently. Through this process, the obtained swollen rubber
 7 sample is a gel-like material with aromatic oils inside the rubber network. Since the geometry of cylindrical
 8 rubber samples changed after swelling, a special drill tool with an inner diameter of 8 mm was used to trim
 9 the swollen sample into the desired diameter. Due to the good adhesion between the plates and swollen
 10 rubber, no glue was used. For both dry and swollen rubber samples, manual adjustment was applied on the
 11 gap between the plates until the normal force is close to zero.

12 Frequency sweep tests of rubber samples were performed from 0.1 to 100 rad/s over a temperature range of
 13 -10~130 °C with an increment of 20 °C. According to the previous study, the measurements were carried
 14 out at a strain level of 1% under strain-controlled mode (22). The viscoelastic parameters (complex modulus
 15 and phase angle) of each sample were collected and analyzed.

16 **Effect of Swelling on the Mechanical Properties of Rubber**

17 From a micromechanics point of view, CRMB can be treated as a composite material in which rubber
 18 particles are included in the bitumen matrix. The change in properties of rubber after swelling has an
 19 important effect on the mechanical properties of rubber modified binders. During the rubber swelling test
 20 process, it was found the swollen rubber sample became soft and viscous due the absorption of bitumen
 21 components, forming a gel-like structure (8; 23). However, few studies have looked into the mechanical
 22 properties of this gel-like material. To further investigate the effect of swelling on the mechanical properties
 23 of rubber, the dry and swollen rubber samples after 36 h interaction at different temperatures were tested by
 24 DSR.

25 Based on the time-temperature superposition principle, the master curves of complex modulus and phase
 26 angle of different rubber samples at a reference temperature of 30 °C were built in Figure 6. From the
 27 obtained data, it was found the swollen rubber is not a rheologically simple material so that common
 28 rheological models for bitumen are not suitable for it. Therefore, the master curves were established using
 29 a generalized logistic function in Equation 4 (24) and the Williams-Landel-Ferry (WLF) equation (Equation
 30 5) for shift factors fitting to form smooth curves.

$$\log A = \delta + \frac{\alpha}{[1 + \lambda e^{(\beta + \gamma(\log \omega))}]^{1/\lambda}} \quad (4)$$

31 where A is either complex shear modulus or phase angle. δ is the lower asymptote; α is the difference
 32 between the values of upper and lower asymptote; λ , β and γ define the shape between the asymptotes and
 33 the location of the inflection point.

$$\log \alpha_T(T) = \frac{-C_1(T - T_R)}{C_2 + (T - T_R)} \quad (5)$$

34 where C_1 , C_2 = empirically determined constants; T = test temperature; T_R = reference temperature;
 35 $\alpha_T(T)$ = shifting factor.

36 It can be seen that dry rubber exhibits obvious elastic behaviors whose complex modulus and phase angle
 37 are almost frequency independent. However, rubbers after swelling show obvious viscoelasticity. The
 38 complex moduli of swollen rubbers were all lower than the dry rubber in the low frequency range. At high

1 frequencies, the modulus of different samples crossed each other. Based on the existing master curves, it
2 can be anticipated that swollen rubber interacted at 200 °C for 36 h shows the highest modulus at very high
3 frequencies (corresponding to very low temperatures). This is because the absorbed bitumen in the swollen
4 rubber sample plays a more dominant role than rubber and behaves more elastic in the composite at low
5 temperatures. Considering the complex modulus of bitumen used in this study at very high frequencies is
6 higher than rubber (25), the swollen rubber sample containing more bitumen will exhibit higher complex
7 modulus at very high frequencies. At the dry state, rubber polymer chains are entangled or crosslinked to
8 each other, forming tightly folded coils, which contributes to the rubber elasticity. When the rubber polymer
9 chain segments start to absorb bitumen molecules, the folded polymer coils start unfolding, causing the
10 swelling and loosening of the network. Consequently, this polymer network swelling process will decrease
11 the complex modulus at a macroscopic scale. With the increase of interaction temperature, the modulus of
12 swollen rubber decreases while the phase angle increases. This means the viscous component in the swollen
13 rubber increases after the interaction at higher temperatures. It is noteworthy that the phase angles of swollen
14 rubber samples increase with the increase of frequency, which is contradictory to the common behaviors of
15 bitumen. This is the unique nature of rubber polymers. Actually, the phase angle of rubber usually
16 experience an increase stage and then a decrease stage over a large frequency range (26).

17 CONCLUSIONS AND RECOMMENDATIONS

18 This study conducted various laboratory tests to investigate the swelling process of rubber in bitumen. The
19 following conclusions can be drawn:

- 20 • Through FTIR results, no rubber dissolution (or too inconspicuous to be detected) during interaction
21 with naphthenic oil takes place in the temperature range from 160 to 200 °C. This supports that
22 rubber did not dissolve into bitumen in the same temperature range. Aliphatic compounds from
23 bitumen preferentially diffused into rubber during the swelling process.
- 24 • Through bitumen sorption tests, the corrected diffusion coefficients of Pen 70/100 bitumen into
25 truck tire rubber are determined as 15.15×10^{-6} , 37.87×10^{-6} and 109.12×10^{-6} mm²/s at 160, 180
26 and 200 °C, respectively. The diffusion coefficient increases with the increase of temperature in an
27 Arrhenius form.
- 28 • The volume expansion of rubber during swelling was captured by the CT scan images. Rubber
29 swells faster at the earlier stages then the expansion rate slows down. The swelling ratio of rubber
30 increased from 1.97 at 160 °C to 3.03 at 200 °C after 36 h interaction.
- 31 • Through DSR tests, swollen rubber becomes softer comparing to the dry rubber and exhibits
32 obvious viscoelastic behaviors. With the increase of temperature, the softening and viscous effect
33 are more significant.

34 The obtained diffusion coefficients, swelling characteristics and mechanical properties can be further used
35 as the model inputs for both numerical simulation of rubber swelling process and micromechanical models
36 to better predict the mechanical performance of CRMB (27). Further research can be extended to more
37 material combinations, e.g., bitumen with different chemical compositions and car tire rubber.

38

39 ACKNOWLEDGMENTS

40 The corresponding author would like to thank the financial support from China Scholarship Council. The
41 financial support of Khalifa University via the CIRA-2018-115 research grant is also gratefully
42 acknowledged.

43

44 AUTHOR CONTRIBUTION STATEMENT

45 The authors confirm contribution to the paper as follows: study conception and design: Haopeng Wang,

1 Xueyan Liu, Sandra Erkens, Athanasios Skarpas; data collection: Haopeng Wang; analysis and
2 interpretation of results: Haopeng Wang, Xueyan Liu, Panos Apostolidis, Athanasios Skarpas; draft
3 manuscript preparation: Haopeng Wang. All authors reviewed the results and approved the final version of
4 the manuscript.
5

6 **DECLARATION OF CONFLICTING INTERESTS**

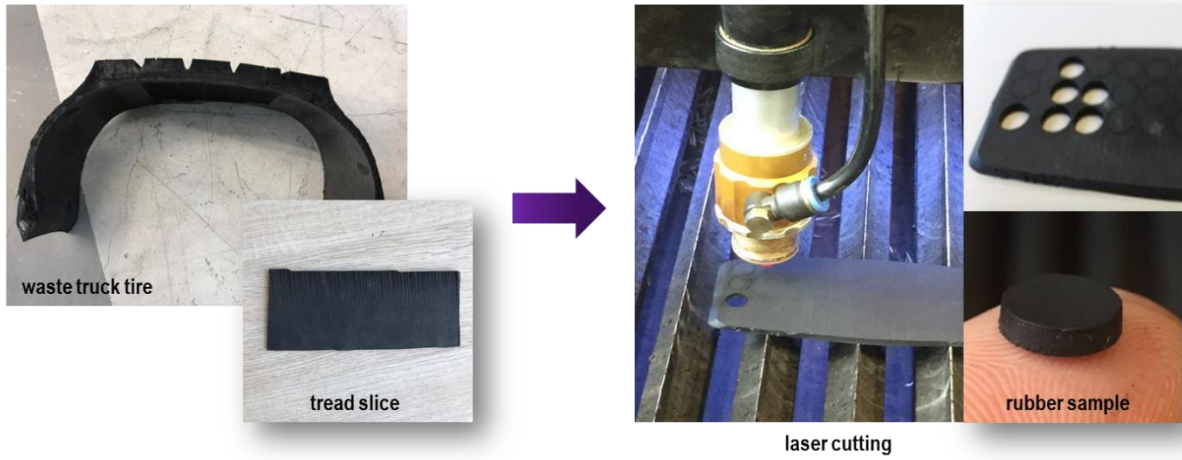
7 The author(s) declared no potential conflicts of interest with respect to the research, authorship, and/or
8 publication of this article.
9

10 **REFERENCES**

- 11 [1] Lo Presti, D. Recycled Tyre Rubber Modified Bitumens for road asphalt mixtures: A literature review.
12 *Construction and Building Materials*, Vol. 49, 2013, pp. 863-881.
13 [2] Shu, X., and B. S. Huang. Recycling of waste tire rubber in asphalt and portland cement concrete: An
14 overview. *Construction and Building Materials*, Vol. 67, 2014, pp. 217-224.
15 [3] Wang, H., X. Liu, P. Apostolidis, and T. Scarpas. Review of warm mix rubberized asphalt concrete:
16 Towards a sustainable paving technology. *Journal of Cleaner Production*, Vol. 177, 2018, pp. 302-314.
17 [4] Lesueur, D. The colloidal structure of bitumen: consequences on the rheology and on the mechanisms
18 of bitumen modification. *Adv Colloid Interface Sci*, Vol. 145, No. 1-2, 2009, pp. 42-82.
19 [5] Asaro, L., M. Gratton, S. Seghar, and N. Ait Hocine. Recycling of rubber wastes by devulcanization.
20 *Resources, Conservation and Recycling*, Vol. 133, 2018, pp. 250-262.
21 [6] Lo Presti, D., and G. Airey. Tyre rubber-modified bitumens development: the effect of varying
22 processing conditions. *Road Materials and Pavement Design*, Vol. 14, No. 4, 2013, pp. 888-900.
23 [7] Ragab, M., M. Abdelrahman, and A. Ghavibazoo. Performance Enhancement of Crumb Rubber-
24 Modified Asphalts Through Control of the Developed Internal Network Structure. *Transportation Research*
25 *Record: Journal of the Transportation Research Board*, Vol. 2371, 2013, pp. 96-104.
26 [8] Wang, H., X. Liu, H. Zhang, P. Apostolidis, T. Scarpas, and S. Erkens. Asphalt-rubber interaction and
27 performance evaluation of rubberised asphalt binders containing non-foaming warm-mix additives. *Road*
28 *Materials and Pavement Design*, 2018, pp. 1-22.
29 [9] Abdelrahman, M. A., and S. H. Carpenter. Mechanism of the interaction of asphalt cement with crumb
30 rubber modifier. *Transportation Research Record: Journal of the Transportation Research Board*, Vol. 1661,
31 1999, pp. 106-113.
32 [10] Zanzotto, L., and G. Kennepohl. Development of rubber and asphalt binders by depolymerization and
33 devulcanization of scrap tires in asphalt. *Transportation Research Record: Journal of the Transportation*
34 *Research Board*, No. 1530, 1996, pp. 51-58.
35 [11] Frantzis, P. Crumb rubber-bitumen interactions: Diffusion of bitumen into rubber. *Journal of materials*
36 *in civil engineering*, Vol. 16, No. 4, 2004, pp. 387-390.
37 [12] Artamendi, I., and H. A. Khalid. Diffusion kinetics of bitumen into waste tyre rubber. *Journal of the*
38 *Association of Asphalt Paving Technologists*, Vol. 75, 2006, pp. 133-164.
39 [13] Dong, D., X. Huang, X. Li, and L. Zhang. Swelling process of rubber in asphalt and its effect on the
40 structure and properties of rubber and asphalt. *Construction and Building Materials*, Vol. 29, 2012, pp. 316-
41 322.
42 [14] Levin, M., and P. Redelius. Determination of three-dimensional solubility parameters and solubility
43 spheres for naphthenic mineral oils. *Energy & Fuels*, Vol. 22, No. 5, 2008, pp. 3395-3401.
44 [15] Zhu, J., R. Balieu, and H. Wang. The use of solubility parameters and free energy theory for phase
45 behaviour of polymer-modified bitumen: a review. *Road Materials and Pavement Design*, 2019, pp. 1-22.
46 [16] Ghavibazoo, A., M. Abdelrahman, and M. Ragab. Mechanism of Crumb Rubber Modifier Dissolution
47 into Asphalt Matrix and Its Effect on Final Physical Properties of Crumb Rubber-Modified Binder.
48 *Transportation Research Record: Journal of the Transportation Research Board*, No. 2370, 2013, pp. 92-
49 101.
50

- 1 [17] Medina, J. R., and B. S. Underwood. Micromechanical shear modulus modeling of activated crumb
2 rubber modified asphalt cements. *Construction and Building Materials*, Vol. 150, 2017, pp. 56-65.
- 3 [18] Gawel, I., R. Stepkowski, and F. Czechowski. Molecular interactions between rubber and asphalt.
4 *Industrial & Engineering Chemistry Research*, Vol. 45, No. 9, 2006, pp. 3044-3049.
- 5 [19] Wang, H., X. Liu, P. Apostolidis, S. Erkens, and T. Scarpas. Numerical investigation of rubber swelling
6 in bitumen. *Construction and Building Materials*, Vol. 214, 2019, pp. 506-515.
- 7 [20] Brown, W., R. Jenkins, and G. Park. The sorption and diffusion of small molecules in amorphous and
8 crystalline polybutadienes. In *Journal of Polymer Science: Polymer Symposia*, No. 41, Wiley Online Library,
9 1973. pp. 45-67.
- 10 [21] Rubinstein, M., and R. H. Colby. *Polymer physics*. Oxford university press New York, 2003.
- 11 [22] Zegard, A., F. Helmand, T. Tang, K. Anupam, and A. Scarpas. Rheological properties of tire rubber
12 using dynamic shear rheometer for fem tire-pavement interaction studies. Presented at 8th International
13 Conference on Maintenance and Rehabilitation of Pavements, Singapore, 2016.
- 14 [23] Xu, B., X. Di, and G. B. McKenna. Swelling Behavior of Cross-Linked Rubber: Explanation of the
15 Elusive Peak in the Swelling Activity Parameter (Dilational Modulus). *Macromolecules*, Vol. 45, No. 5,
16 2012, pp. 2402-2410.
- 17 [24] Rowe, G., G. Baumgardner, and M. Sharrock. Functional forms for master curve analysis of bituminous
18 materials. *Advanced Testing and Characterisation of Bituminous Materials, Vols 1 and 2*, 2009, pp. 81-+.
- 19 [25] Wang, H., X. Liu, P. Apostolidis, and T. Scarpas. Rheological Behavior and Its Chemical Interpretation
20 of Crumb Rubber Modified Asphalt Containing Warm-Mix Additives. *Transportation Research Record:
21 Journal of the Transportation Research Board*, Vol. 2672, No. 28, 2018, pp. 337-348.
- 22 [26] Santangelo, P. G., and C. M. Roland. Temperature Dependence of Mechanical and Dielectric Relaxation
23 incis-1,4-Polyisoprene. *Macromolecules*, Vol. 31, No. 11, 1998, pp. 3715-3719.
- 24 [27] Wang, H., X. Liu, H. Zhang, P. Apostolidis, S. Erkens, and A. Skarpas. Micromechanical modelling of
25 complex shear modulus of crumb rubber modified bitumen. *Materials & Design*, Vol. 188, 2020.
- 26
- 27

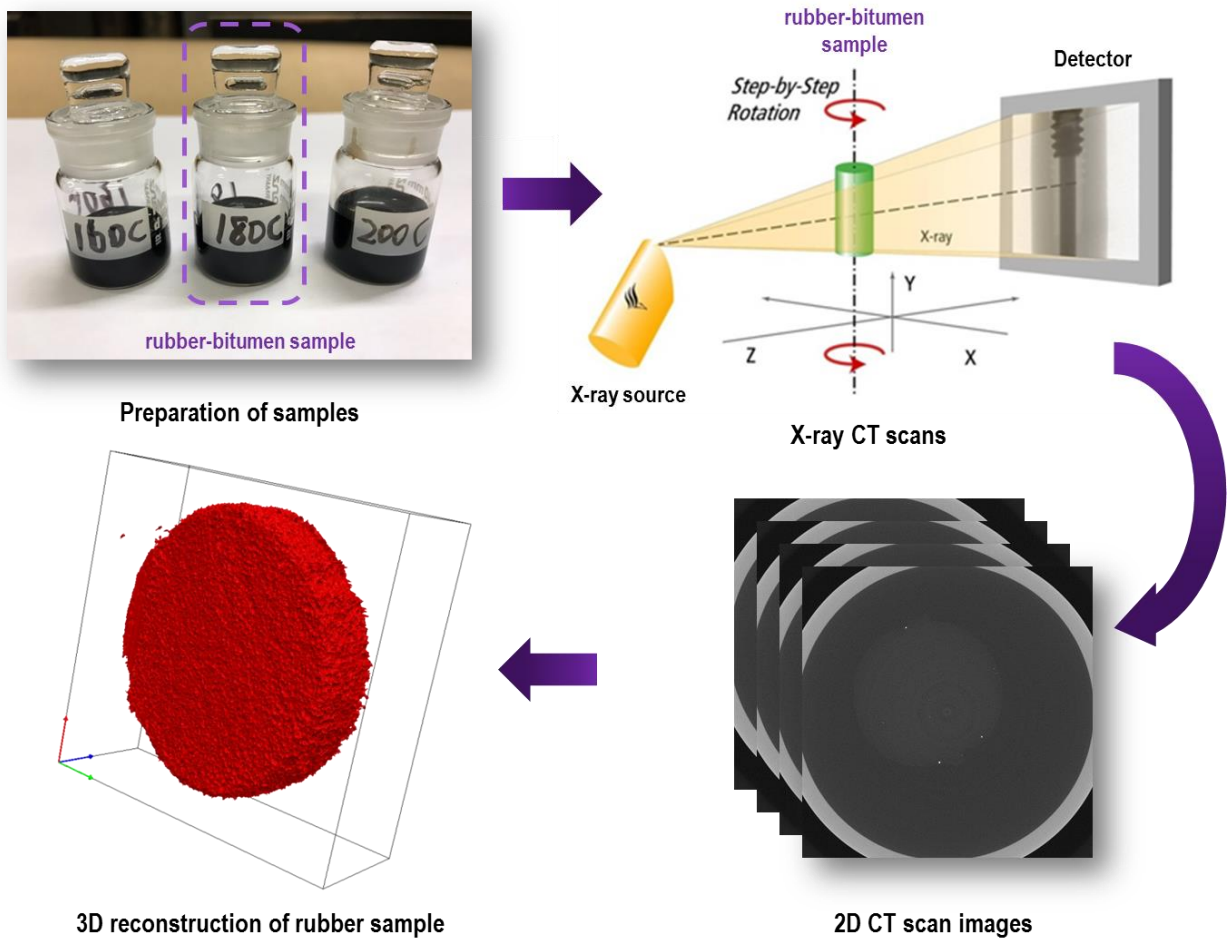
1



2

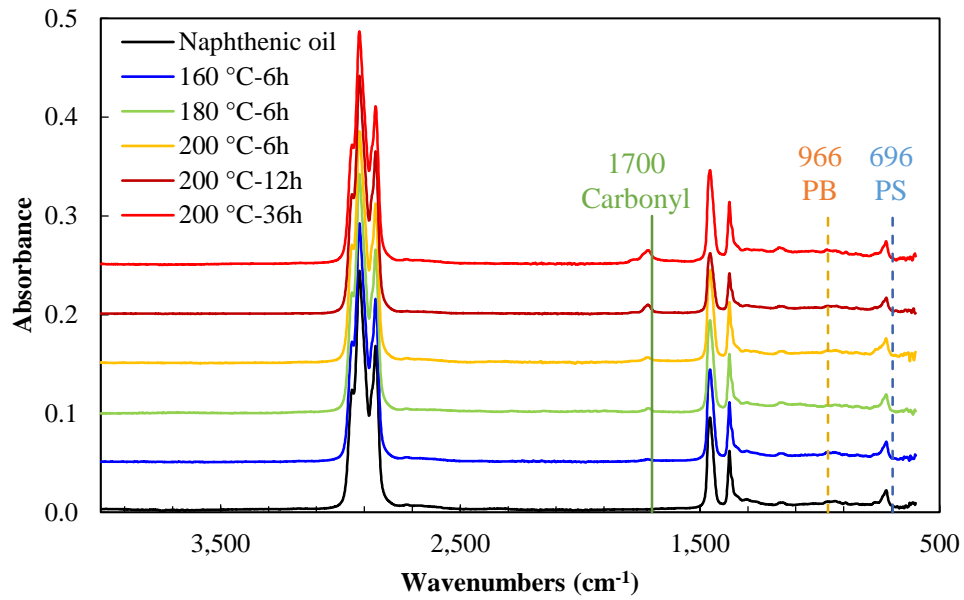
3 **Figure 1.** Cylindrical rubber sample (2 mm-thickness and 8 mm-diameter) preparation process.

4



5

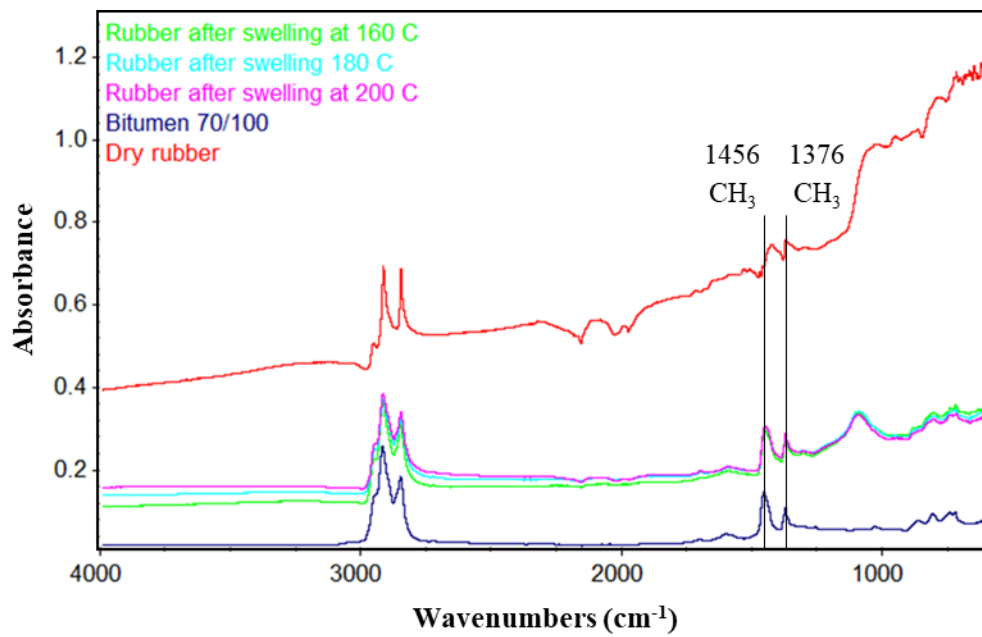
6 **Figure 2.** X-ray CT scan test for monitoring the rubber swelling process.



1

2

(a)

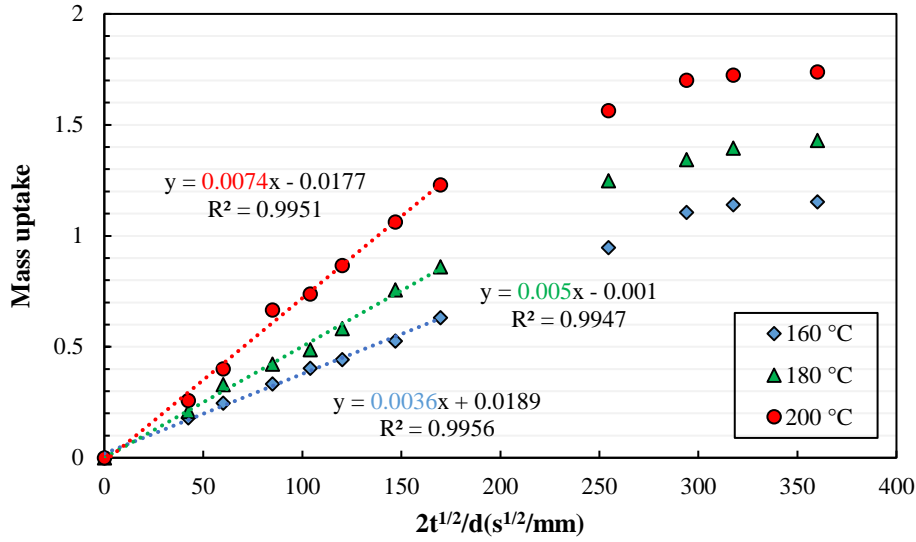


3

4

(b)

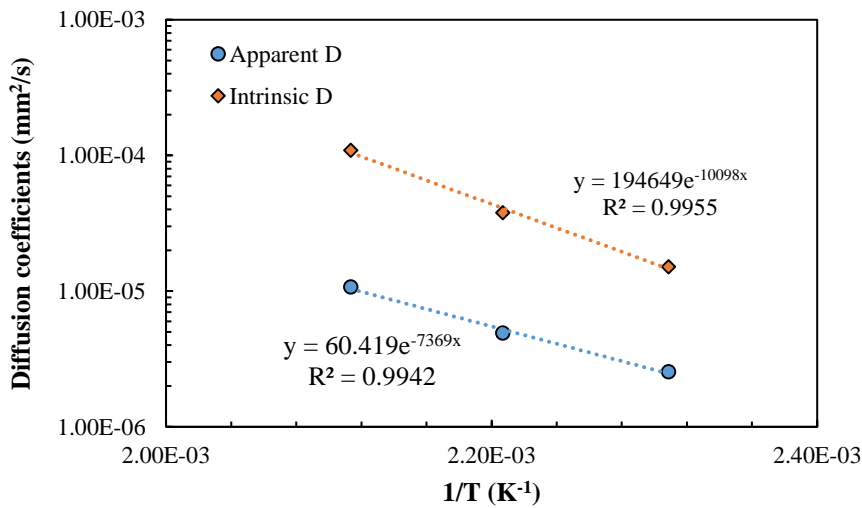
5 **Figure 3.** FTIR results of (a) reacted naphthenic oil samples and (b) rubber samples before and after swelling.



1

2

(a)



3

4

(b)

5 **Figure 4.** (a) Sorption curves of bitumen into truck tire rubber (b) Temperature dependence of the diffusion
6 coefficients.

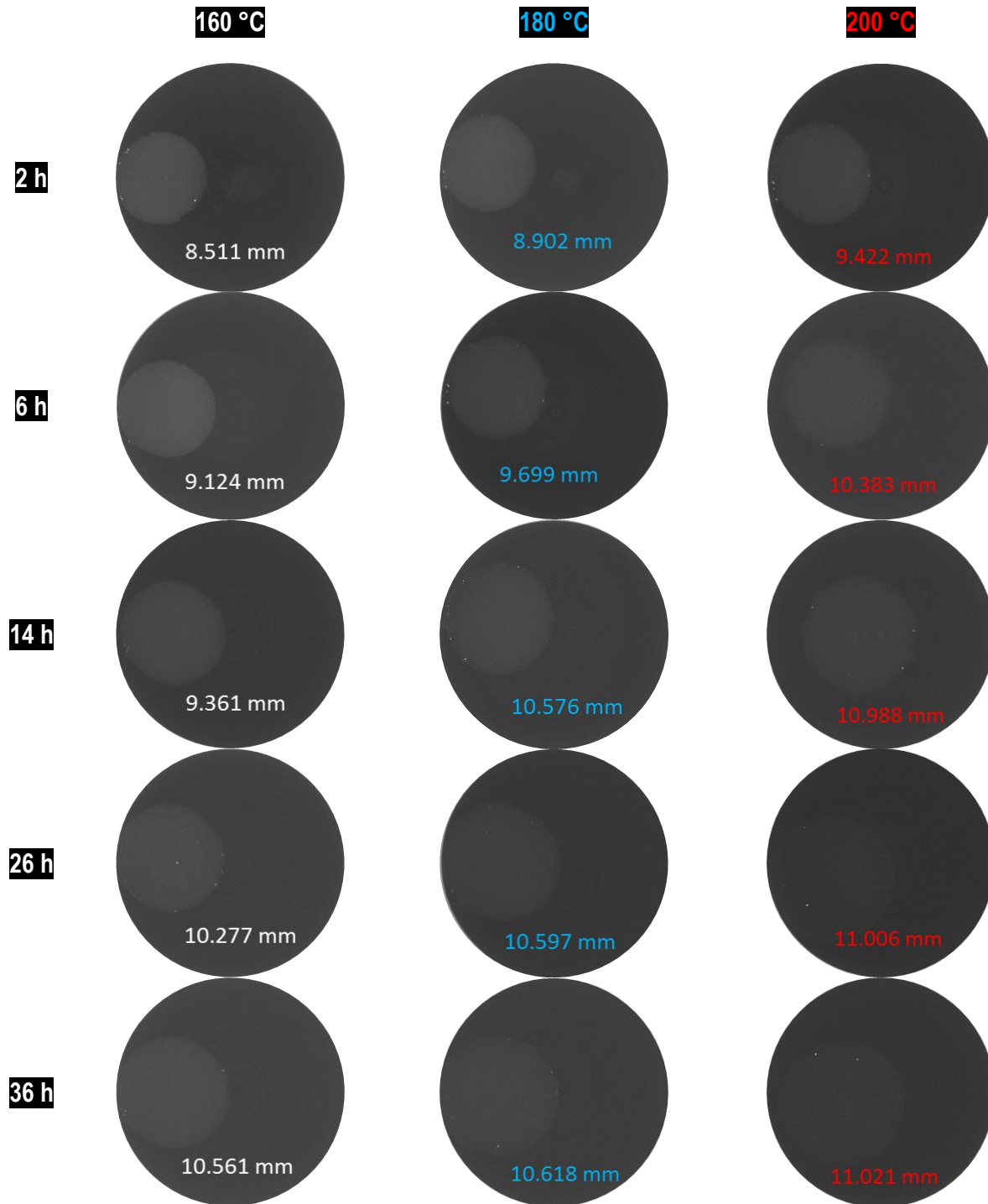
7

8

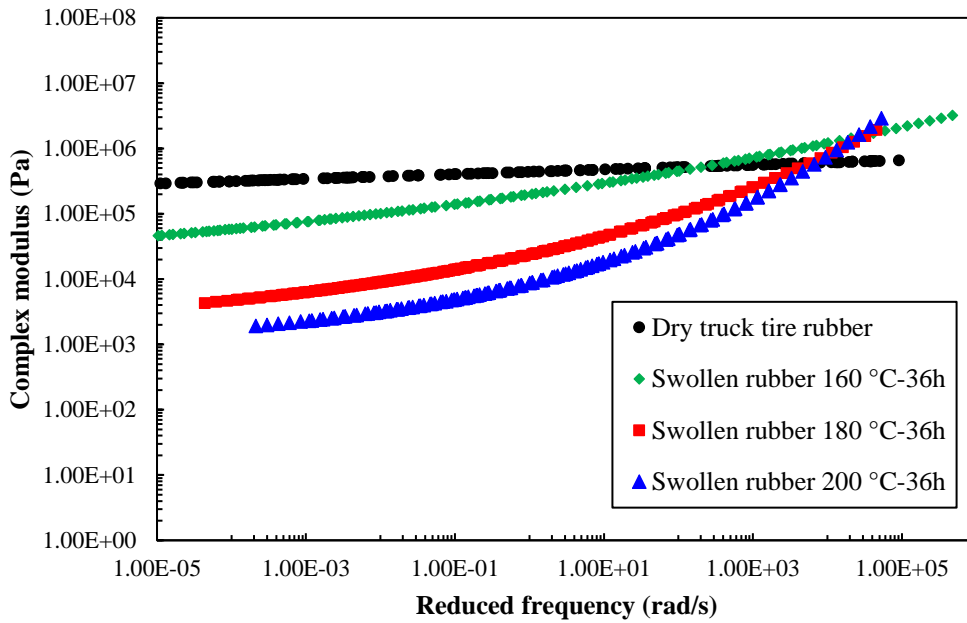
9

10

11



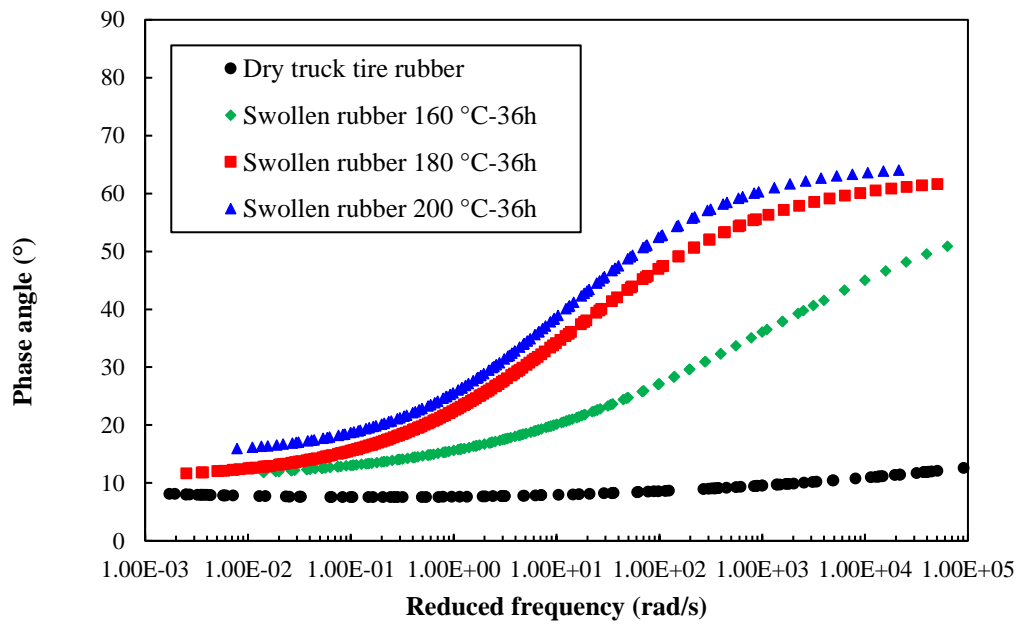
1 **Figure 5.** 2D slice images from CT scan at different interaction temperatures and times.



1

2

(a)



3

4

(b)

Figure 6. (a) Complex modulus and (b) phase angle master curves of rubber before and after swelling.

6

7

8

1 **Table 1.** Diffusion coefficients and equilibrium mass uptake of bitumen into truck tire rubber.

Temperature (°C)	Equilibrium $(M_t - M_0)/M_0$	$D \times 10^{-6}$ (mm ² /s)	ϕ	$D^* \times 10^{-6}$ (mm ² /s)
160	1.15	2.54	0.465	15.15
180	1.40	4.91	0.417	37.87
200	1.70	10.75	0.370	109.12

2

3 **Table 2.** Derived volumes of swollen rubbers through 3D reconstruction at different interaction conditions.

Time (h)	Volume (mm ³)		
	160 °C	180 °C	200 °C
0	100.5	100.5	100.5
2	116.2	129.1	177.2
6	138.4	156.3	239.5
14	157.1	190.6	287.4
26	169.2	236.5	301.3
36	197.6	247.7	304.6

4